



Article

Research on the Longitudinal and Transverse Coupling Dynamic Behavior and Yaw Stability of an Articulated Electric Bus

Jinxiang Song¹, Honglei Qi^{1,*}, Zebin Li¹, Shiqi Liu¹, Ze Ren²  and Qiang Wang^{1,2} 

¹ Zhongtong Bus Holding Co., Ltd., Liaocheng 252000, China; songjx@zhongtong.com (J.S.); lizb904@zhongtong.com (Z.L.); liusq@zhongtong.com (S.L.); wangqiang@sdust.edu.cn (Q.W.)

² School of Transportation, Shandong University of Science and Technology, Qingdao 266000, China; 202382160030@sdust.edu.cn

* Correspondence: qihl@zhongtong.com

Abstract: The dynamic behaviors of articulated buses during braking and steering processes are exceedingly complex due to the transmission of various forces and torques by the articulated device. The coupling of forces between the front and rear carriages often renders the bus prone to yaw instability under extreme operating conditions. In this paper, according to the characteristics of the structure and parameter matching of an electrically driven articulated bus, a dynamic model of longitudinal and transverse coupling applied on an articulated bus is established, and the influence of the articulated structure on the yaw stability of the drive vehicle is analyzed. Combined with the relationship between the driving motor, the hinge device, and the vehicle motion, a cruise simulation model of the bus is developed, enabling a comparative analysis and verification of vehicle stability under typical road conditions. The results offer a theoretical foundation for the design and control of highly reliable articulated buses.

Keywords: articulated bus; articulated device; longitudinal and transverse coupling dynamic



Citation: Song, J.; Qi, H.; Li, Z.; Liu, S.; Ren, Z.; Wang, Q. Research on the Longitudinal and Transverse Coupling Dynamic Behavior and Yaw Stability of an Articulated Electric Bus. *Energies* **2024**, *17*, 2449. <https://doi.org/10.3390/en17112449>

Academic Editors: Peter Gaspar and Junnian Wang

Received: 2 April 2024

Revised: 11 May 2024

Accepted: 13 May 2024

Published: 21 May 2024



Copyright: © 2024 by the authors. Licensee MDPI, Basel, Switzerland. This article is an open access article distributed under the terms and conditions of the Creative Commons Attribution (CC BY) license (<https://creativecommons.org/licenses/by/4.0/>).

1. Introduction

Articulated buses have been widely used in urban traffic in many large- and medium-sized cities in China, favored for their expansive internal space and robust adaptability to varied pavements. However, the dynamic behaviors of articulated buses during the braking and steering processes are exceedingly complex because of the articulated devices. Moreover, due to the coupling of the forces between the front and rear carriages, the articulated bus is prone to yaw instability under extreme operating conditions. Therefore, the research on the handling stability of articulated buses under complex operating conditions is the key to the high reliability and efficient control design of articulated electric buses.

In recent years, the dynamic modeling of articulated buses during the braking and steering process has attracted extensive attention from scholars. The transverse dynamics of multi-axle and multi-articulated vehicles have been analyzed, and with that, a linear planar dynamic model of an articulated vehicle came to be established [1]. The authors of [2] established a simplified model for the yaw and roll of articulated buses and corrected the key parameters of the simplified model based on the real-time state of the vehicle. In [3], Shen et al. proposed a rigid differential steering mode for articulated vehicles and analyzed the vehicle steering behavior in a composite steering mode with hydraulic steering as the main method and differential steering as the auxiliary method. The dynamic model for each subsystem of articulated loaders was established. In addition, the vehicle mechanical dynamics and steering behaviors under predetermined paths were provided in [4]. A polyhedral vehicle model considering uncertain parameters was established, and the active trailer steering behaviors of multi-trailer articulated heavy vehicles were studied [5]. Combined with the nonlinear yaw model of the articulated dump truck, Rakheja et al. [6] established the kinematic and dynamic model of the steering mechanism of the vehicle

frame. In addition, the influence of the change in the effective damping applied to the steering mechanism on the response of the steering system under stable steering and pulse steering input has been researched. A dynamic model for the hydraulic steering system of articulated heavy vehicles was established, and the performance of the vehicle steering was analyzed [7]. A Jacobian linearized kinematics model of an articulated vehicle based on the geometric structure characteristics of articulated vehicles was established, and the steering motion performance of an articulated vehicle was studied [8]. A vehicle motion model considering body roll and centroid bias was established, and the effect of the centroid bias in the front and rear carriages on the vehicle handling stability was discussed [9].

To solve the problem of the braking stability of articulated buses, scholars have conducted thorough research. A verified nonlinear dynamic model of a tractor–semi-trailer was established, and the vehicle slip response under emergency braking conditions was studied [10]. Aiming at the problems of insufficient braking force, collision, and folding in the braking process of articulated vehicles, a kind of eddy current retarded axle was designed, and a braking dynamic model of an articulated vehicle was established in [11]. Based on the articulated vehicle dynamics model, the influence of the participation of the braking system on the lateral stability control was analyzed when the steering actuator performance decreased [12]. As can be observed in the studies by Nie et al. [13], the braking force variation of the articulated vehicle under different control modes was revealed according to the five-degrees-of-freedom simplified articulated vehicle dynamics model. Zhang et al. [14] took the six-axle articulated train as a research object and gave the speed characteristics of an articulated vehicle during the long downhill braking process. The yaw stability of articulated passenger cars is very important for vehicle driving safety; for this reason, in [15], Huang et al. adopted the reconfigurable method to establish a comprehensive model of the yaw dynamics of passenger cars with arbitrary axles or articulated structures. A linear three-degrees-of-freedom reference model for multi-axle wheel-driven articulated passenger cars was established, and the possible phenomena of folding, tail flick, and yaw in extreme working conditions were analyzed [16]. In [17], Yang et al. established a two-degree-of-freedom mathematical model of a multi-axle heavy-duty launch vehicle and used a co-simulation method to study the yaw motion behavior of the vehicle. A nonlinear dynamic model and a hydraulic steering system model of an articulated vehicle were established, and the handling stability of the vehicle in a detour was discussed in [18]. Another nonlinear dynamic model of a traction-semi-trailer was established, and the vehicle side-slip motion response under the limit adhesion condition was given in [19]. The studies in [20] showed the nonlinear effects of the changes in steering force caused by large steering angles, nonlinear cornering characteristics, and centrifugal effects on the vehicle lateral dynamics. Based on the dynamic behaviors of articulated vehicles in multibody simulation models with and without suspension, the serpentine stability of articulated vehicles was discussed [21]. Zhu et al. [22] evaluated the lateral stability of articulated steering vehicles based on a data-driven modeling method.

The main contributions of this study are as follows. Firstly, according to the configuration and matching characteristics of the electric articulated bus, the longitudinal and lateral coupling dynamic model of the whole vehicle is established. Secondly, combined with cruise simulation, the influence of the articulated structure on the yaw stability of driving vehicles and the change rule of influence are analyzed. Finally, through a simulation under typical road conditions, the stability of the driving bus is compared and verified.

2. External Driving Characteristics of an Articulated Bus

The determination principle for the total power requirement of an articulated bus is similar to that of a traditional bus, both of which are determined according to the power performance of the whole vehicle. Usually, the maximum power of the drive motor is determined by the highest speed, the acceleration performance index, and the maximum gradeability. The power design flow of the power system is shown in Figure 1.

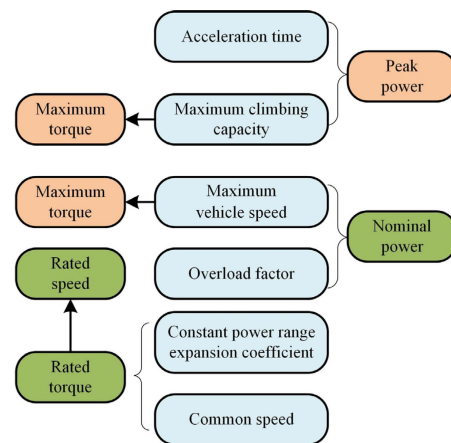


Figure 1. Design process of the power system of articulated buses.

The rated torque of the power system of articulated buses must meet the power performance index, which usually refers to the requirements of the maximum climbing capacity and target working conditions of the vehicle. The rated torque T_e of the drive motor is proportional to the rated speed n_e . The conversion relationship is expressed as follows:

$$T_e = 9550 \frac{P_e}{n_e} \quad (1)$$

This paper researches a triaxial two-axle drive articulated passenger car. The external characteristic curve of the drive motor is selected through testing, as shown in Figure 2, and the power map distribution of the drive motor is given, as shown in Figure 3.

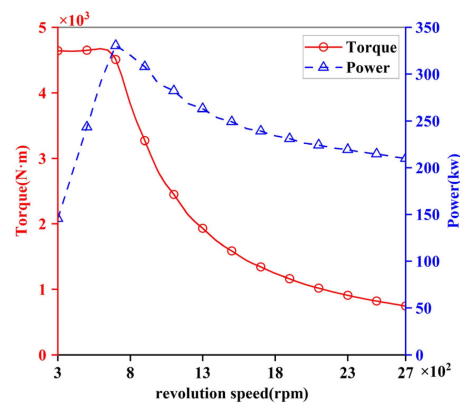


Figure 2. The external characteristic curve of the drive motor.

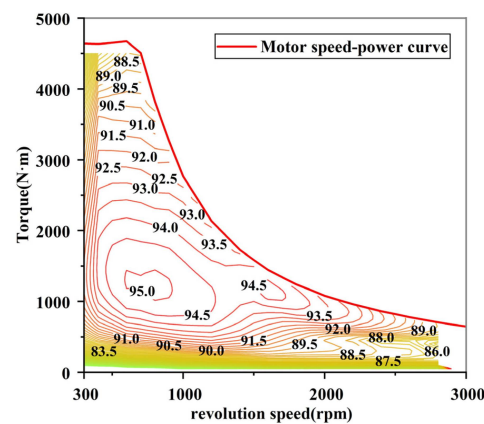


Figure 3. Power map distribution of drive motor.

3. Modeling of Longitudinal and Transverse Coupling Dynamics

An articulated bus is a multi-degree-of-freedom spatial motion system with a complex structure. To easily facilitate the study of the dynamic characteristics of an articulated bus, the model was simplified. Some assumptions were made as follows:

1. The front and rear carriages of the articulated bus are regarded as rigid bodies.
2. The influence of the air resistance is not considered.
3. The effect of the load transfer on the tire cornering characteristics is not considered.

The force of the articulated bus was analyzed based on the above assumptions, as shown in Figure 4. The force analysis on the roll motion of the articulated bus is shown in Figure 5.

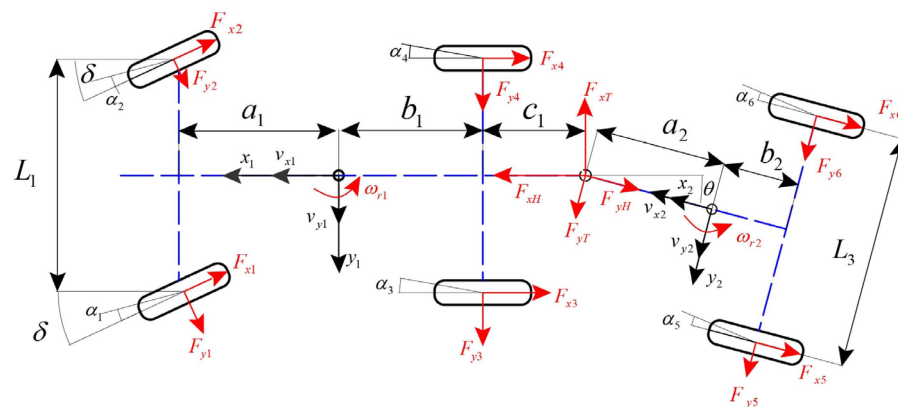


Figure 4. Longitudinal and transverse force analysis of articulated bus.

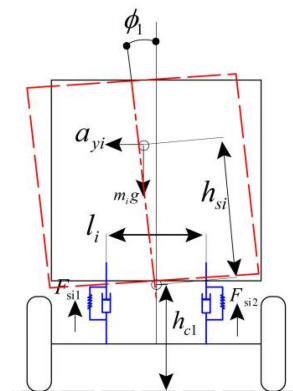


Figure 5. Force analysis diagram of roll motion.

The front and rear carriages of the articulated bus are hinged by the hinge plate, influencing each other during the driving process, making it crucial to analyze the hinged part of the articulated passenger car.

The longitudinal external force and longitudinal motion equations of the front carriage are as follows:

$$m_1(\dot{x}_1 + v_{y1}\omega_{r1}) = \begin{aligned} &-(F_{x1} + F_{x2}) \cos \delta \\ &-(F_{y1} + F_{y2}) \sin \delta \\ &-F_{x3} - F_{x4} + F_{xH} \end{aligned} \quad (2)$$

$$m_1(\dot{v}_{y1} + v_{x1}\omega_{r1}) = \begin{aligned} &-(F_{x1} + F_{x2}) \sin \delta \\ &+(F_{y1} + F_{y2}) \cos \delta \\ &+F_{y3} + F_{y4} - F_{yH} \end{aligned} \quad (3)$$

The lateral external force and lateral motion equation of the front carriage is given as follows:

$$m_1(\dot{v}_{y1} + v_{x1}\omega_{r1}) = -(F_{x1} + F_{x2})\sin\delta + (F_{y1} + F_{y2})\cos\delta + F_{y3} + F_{y4} - F_{yH} \quad (4)$$

The equation of the longitudinal external force and longitudinal motion of the rear carriage is described as

$$m_2(\dot{v}_{x2} - v_{y2}\omega_{r2}) = -F_{xT} + F_{-x5}F_{x6} \quad (5)$$

The lateral external force and lateral motion equation of the rear carriage is expressed as follows:

$$m_2(\dot{v}_{y2} + v_{x2}\omega_{r2}) = F_{yT} + F_{+y5}F_{y6} \quad (6)$$

The yaw external moment and yaw motion equation of the front carriage can be obtained as

$$\begin{aligned} I_{x1}\dot{\omega}_{p1} &= (F_{x1} - F_{x2})\cos\delta \cdot \frac{L_1}{2} - m_1gh_{s1}\sin\varphi_1 \\ &+ (F_{x1} - F_{x2})\sin\delta \cdot a_1 + (F_{x3} - F_{x4}) \cdot \frac{L_2}{2} \\ &+ (F_{y1} - F_{y2})\frac{L_1}{2}\sin\delta + (F_{y2} - F_{y1})a_1\cos\delta \\ &- (F_{y3} + F_{y4}) \cdot b_1 + F_{yH}(b_1 + c_1) \\ &- m_1h_{s1}(\dot{v}_{y1} + v_{x1}\omega_{p1})\cos\varphi_1 \end{aligned} \quad (7)$$

The roll external torque and roll motion equation of the front compartment is designed as follows:

$$\begin{aligned} I_{x1}\dot{\omega}_{p1} &= (F_{si1} - F_{si2})\cos\varphi_1 \cdot \frac{l_1}{2} \\ &+ (F_{si1} - F_{si2})\cos\varphi_1 + F_{yH}(h_{c1} - h_3) \\ &- m_1h_{s1}(\dot{v}_{y1} + v_{x1}\omega_{p1})\cos\varphi_1 - m_1gh_{s1}\sin\varphi_1 \end{aligned} \quad (8)$$

The yaw external moment and yaw motion equation of the rear carriage can be obtained as

$$I_{x2}\dot{\omega}_{r2} = (F_{x5} - F_{x6})\frac{L_3}{2} - (F_{y5} - F_{y6})b_2 - F_{yT} \cdot a_2 \quad (9)$$

The roll external torque and roll motion equation of the rear compartment is designed as follows:

$$\begin{aligned} I_{x2}\dot{\omega}_{p2} &= (F_{s31} - F_{s32})\frac{l_3}{2}\cos\varphi_2 \\ &+ F_{yT}(h_{c2} - h_3) - m_2gh_{s2}\sin\varphi_2 \\ &- m_2h_{s2}(\dot{v}_{y2} + v_{x2}\omega_{p2})\cos\varphi_2 \end{aligned} \quad (10)$$

The relationship between the longitudinal force and the lateral force coordinate at the hinged joint can be obtained as

$$\begin{cases} F_{xH} = F_{yT}\sin\theta - F_{xT}\cos\theta \\ F_{yH} = F_{xT}\sin\theta - F_{yT}\cos\theta \end{cases} \quad (11)$$

where F_{xH} and F_{yH} are the longitudinal hinge force and lateral hinge force of the tractor, respectively. F_{xT} and F_{yT} are the longitudinal hinge force and lateral hinge force of the rear carriage, respectively. θ is the hinge angle.

The velocity coupling equation at the hinged joint is

$$\begin{cases} v_{x2} = v_{x1}\cos\theta - [v_{y1} - \omega_{r1}(b_1 + c_1)]\sin\theta \\ v_{y2} = v_{x1}\sin\theta - [v_{y1} - \omega_{r1}(b_1 + c_1)]\cos\theta - a_2\omega_{r2} \end{cases} \quad (12)$$

$$\dot{\theta} = \omega_{r1} - \omega_{r2} \quad (13)$$

4. Typical Road Condition Simulation and Verification

Based on the longitudinal and transverse coupling dynamic model of an articulated bus, a simulation model was constructed using Cruise simulation software, as shown in Figure 6.

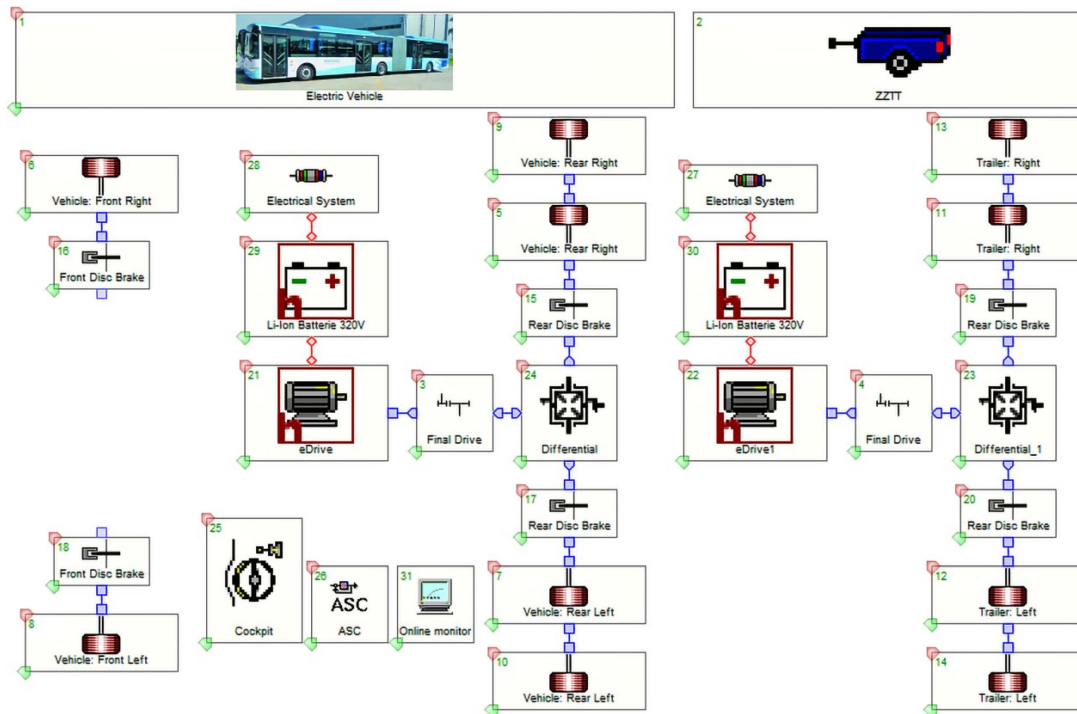


Figure 6. Cruise simulation model diagram.

4.1. J-Type Road

We tested the driving condition of the whole vehicle after the driver provided a large turning angle, including wheel slip and vehicle rollover stability, etc., in which the vehicle response body posture angle, yaw angle, and roll angle are important output curves. When the whole vehicle is driven at 45 km/h, the input corner data curve is shown as follows.

In Figure 7, the driver's steering wheel angle is rotated counterclockwise to $+294^\circ$ and kept for 0.25 s; then, it is rotated clockwise to -294° and kept for 2.5 s, and the steering wheel is reset. Finally, the steering wheel angle is kept unchanged. This operation simulated the turning condition of the bus on a narrow road, and the vehicle data are obtained as shown in Figure 8.

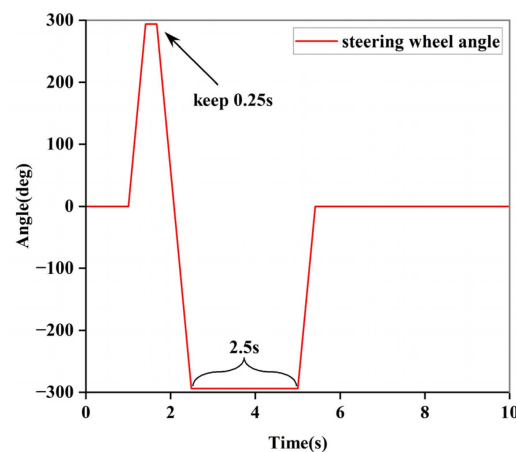


Figure 7. Driver input steering angle.

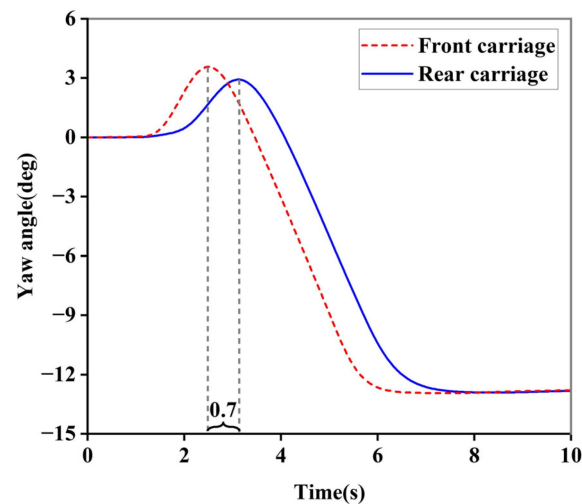


Figure 8. Yaw angle variation curve and the target curve.

After the steering wheel angle is entered by the driver, the first reaction is the front carriage. The front carriage produces the yaw angle and drives the rear carriage to turn. The sequence is fixed; the yaw angle of the front carriage is larger than that of the rear carriage, and the change in the yaw angle at the end of the turn also follows the above law.

Figure 9 shows the cornering angle curve of the vehicle. Since the steering of the vehicle in the driving process will cause the centroid deflection, the sideslip angle is reflected on the car body. The appearance of the sideslip angle of the front carriage is earlier than that of the rear carriage. In addition, the sideslip angle of the front carriage at the wave peak is larger. At 4.5 s, the sideslip angle of the rear carriage is larger than that of the front carriage. The roll angle requires that the roll angle of the car body be less than 3° , since the roll angle is related to the lateral acceleration when the bus drives at a constant circle speed with a centripetal acceleration of 0.4 g. Generally speaking, the roll angle of the car body is measured by the roll gradient. Usually, the lateral angle of the vehicle is kept within 2.5° . In summary, the articulated bus mentioned in this report meets the requirements of the national standard.

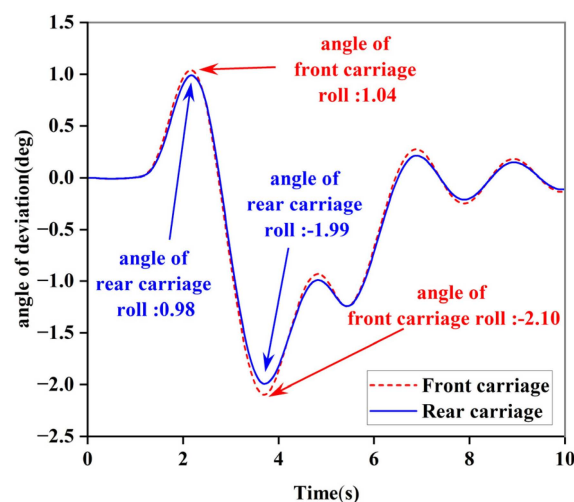


Figure 9. Cornering angle curve of front and rear compartments.

Figure 10 shows the driving path of the whole vehicle; the blue curve is the path of the front carriage, and the red dotted line represents the driving path of the rear carriage. The curves of the front and rear carriages are smooth when turning, and there is no tail flick phenomenon.

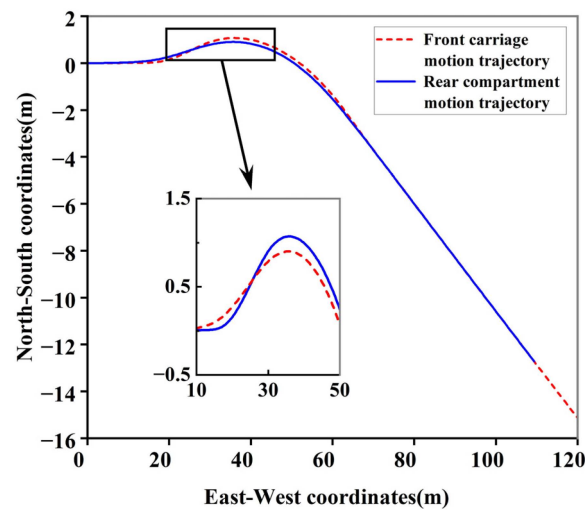


Figure 10. Vehicle driving path tracking map.

4.2. Ring Road

This simulation mainly analyzed the dynamic performance and braking performance of the bus during turning. The initial setting was in a ring road with a diameter of 305 m, and the vehicle speed was set at 60 km/h, which reached the maximum speed of the bus after 20 s of a static start, and then braked. The speed conditions are shown in Figure 11.

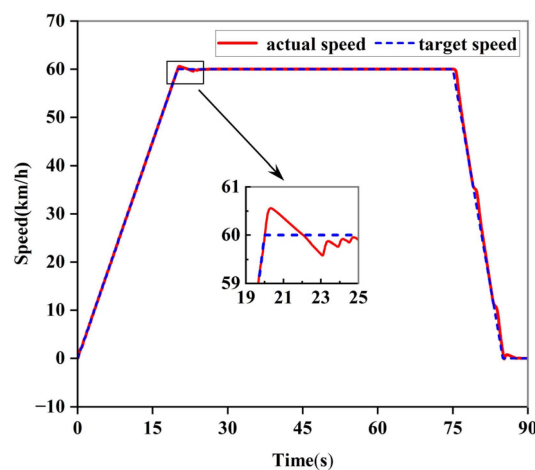


Figure 11. Vehicle target speed versus actual speed curve.

In Figure 11, the target speed curve basically coincides with the actual speed curve. There is a speed peak when the vehicle is accelerated to the highest speed, and then the speed converges to 60 km/h. The speed cannot reach a normal level in driving conditions, and the reason is related to the simulation path. When the bus runs on a circular road, the front carriage can be steered because the front wheels are steering wheels, but the steering of the rear carriage can only rely on the traction of the front carriage. Therefore, the driving force direction of the rear carriage should be on the tangent of the driving path during the driving process. There will be a small fluctuation in the speed of the whole vehicle, which is within 0.1 km/h and has little impact on the actual operation of the whole vehicle. The vehicle can reach the maximum speed in about 20 s on the ring road, and the power system of the whole vehicle is also verified. Its engine can meet the requirements of whole vehicle performance.

Figure 12 shows the path tracking diagram in the simulation. The red curve is the movement track of the front carriage, and the blue dotted line represents the movement track of the rear carriage. Over the whole driving process, because the front carriage

is affected by the driving force of the rear carriage, the front carriage generates a yaw moment. As the whole path is circular, the yaw moment always exists, resulting in the overall steering curve not fully fitting the target curve, and oversteering is produced. In the follow-up study, the output driving force of the rear compartment can be appropriately reduced when the vehicle turns, which makes the rear compartment produce tension on the hinged disc to achieve the understeer characteristic.

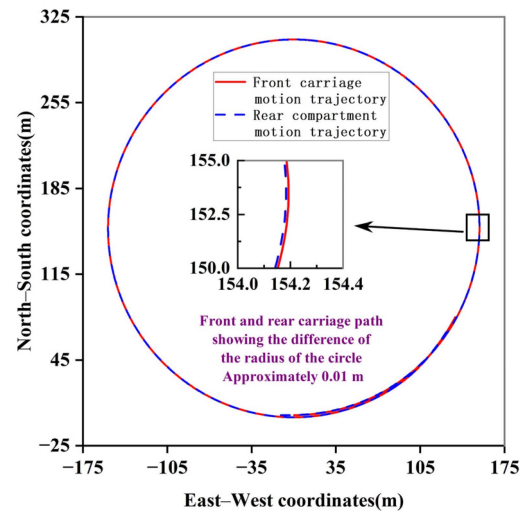


Figure 12. Tracking diagram of bus trajectory.

4.3. Sinusoidal Oscillation Working Condition

Aiming at the influence of the steering wheel jitter on the vehicle driving at high speed, the handling stability of the middle range of the steering wheel rotation angle is the handling stability of the bus at high speed under the condition of a small steering angle and low frequency sine input. The steering radius is a physical parameter to evaluate the flexibility of passenger cars. The steering wheel angle input of a bus driving on a sine curve is a sine oscillation curve; so, when the vehicle speed is kept at 60 km/h, the low amplitude oscillation curve of the steering wheel is shown in Figure 13.

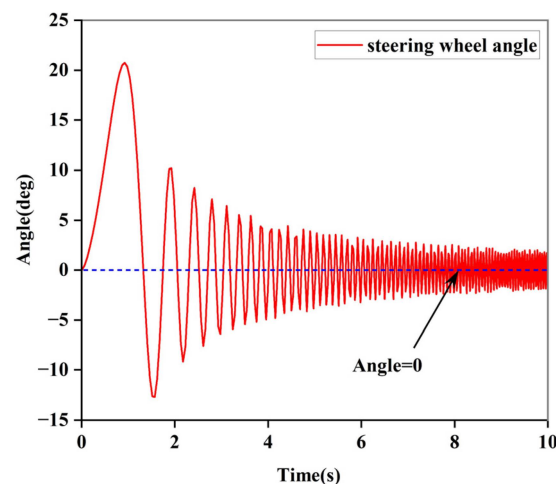


Figure 13. Steering wheel angle curve.

Figure 13 shows the sinusoidal oscillation curve, which is input by the steering wheel. At the beginning, the steering wheel is rotated 20° counterclockwise; then, it is rotated clockwise -15° , and then it is rotated $+10^\circ$ counterclockwise. It is worth noting that the peak value of the steering wheel angle input decreases sequentially. As a large counterclockwise rotation angle is produced at the initial stage of the test, the car body is not aligned by the

subsequent steering; so, the vehicle path will deviate to the left. The acceleration curve is shown in Figure 14.

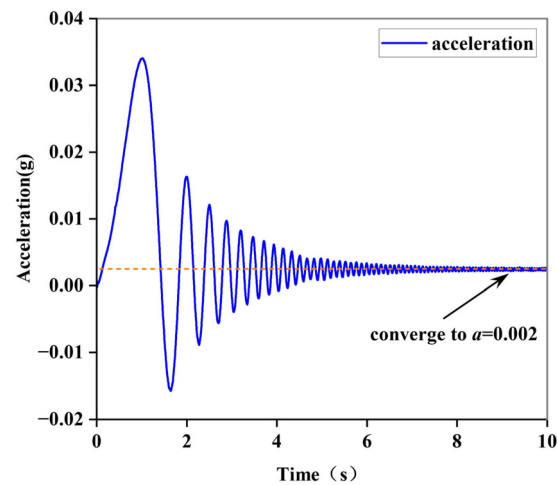


Figure 14. Transverse acceleration curve.

Figure 14 shows that the overall transverse acceleration is above zero and gradually tends to a fixed value, which is related to the driving force of the rear carriage. Because the passenger car is turned to the left, and the yaw amplitude is small, the driving force of the rear carriage cannot be fitted to the driving path curve after the front carriage is turned, resulting in a phenomenon that transverse acceleration always exists. The path tracking of the bus is shown in Figure 15.

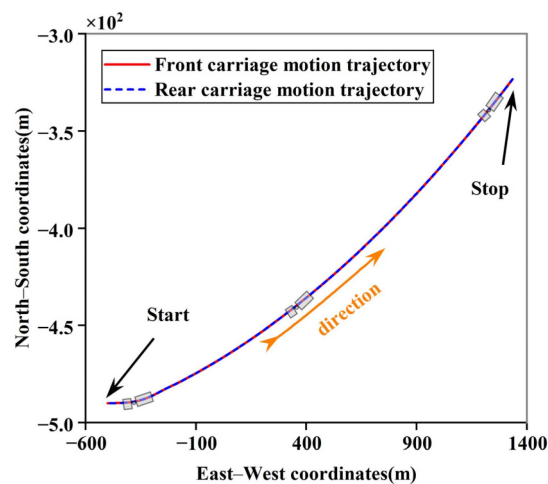


Figure 15. Vehicle path tracking map.

Based on the above simulation curve, it can be seen that the bus route does not shake because of the initial large steering; namely, the small steering wheel oscillation has little effect on the driving state of the whole vehicle, and the bus is still driven in the original direction. However, due to the influence of the driving force, the steering wheel jitter of the bus in the turning state will not make the transverse acceleration become 0, but it will gradually tend to a small fixed value.

5. Conclusions

1. In this paper, according to the characteristics of the structure and parameter matching of the electric drive articulated bus, the parameters of the external characteristics of the vehicle were analyzed. Combined with the external characteristics of the drive motor system and the power map distribution, the longitudinal and lateral coupling

dynamic model of the articulated bus was established, and the longitudinal and lateral coupling dynamic behaviors of the vehicle were analyzed.

2. Combined with the relationship among the driving motor, the hinged device, and the vehicle motion, the simulation model of the electric drive articulated bus was established on the Cruise platform, and the driving stability of the vehicle under typical road conditions was simulated and comparatively analyzed. The analysis of the results verified that the designed articulated bus is in a relatively stable state during the braking process. In addition, the longitudinal and transverse velocities and sideslip angles of the articulated bus are in line with the bus design specifications under the working conditions of J-type road, ring road, and sinusoidal oscillation. The results provide effective theoretical and technical support for the high-reliability design and control of articulated buses.

Author Contributions: Conceptualization, J.S. and Q.W.; methodology, J.S., H.Q. and Q.W.; software, J.S. and Z.L.; validation, J.S. and H.Q.; formal analysis, J.S. and Z.L.; investigation, H.Q.; resources, J.S. and Z.L.; writing—original draft preparation, J.S. and S.L.; writing—review and editing, J.S.; visualization, H.Q.; supervision, Z.R.; project administration, J.S. All authors have read and agreed to the published version of the manuscript.

Funding: This research was funded by the China Postdoctoral Science Foundation, grant number 2022M713655.

Data Availability Statement: The original contributions presented in the study are included in the article, further inquiries can be directed to the corresponding authors.

Conflicts of Interest: Authors Jinxiang Song, Honglei Qi, Zebin Li, Shiqi Liu, Qiang Wang were employed by the company Zhongtong Bus Holding Co., Ltd. The remaining authors declare that the research was conducted in the absence of any commercial or financial relationships that could be construed as a potential conflict of interest.

References

1. Aoki, A.; Marumo, Y.; Kageyama, I. Effects of multiple axles on the lateral dynamics of multi-articulated vehicles. *J. Veh. Syst. Dyn.* **2013**, *51*, 338–359. [\[CrossRef\]](#)
2. Guan, H.; Kim, K.; Wang, B. Comprehensive path and attitude control of articulated vehicles for varying vehicle conditions. *J. Int. J. Heavy Veh. Syst.* **2017**, *24*, 65–95. [\[CrossRef\]](#)
3. Shen, Y.H.; Niu, T.W.; Liu, Z.X. Energy saving analysis of electro-hydraulic compound steering mode of distributed drive articulated vehicle. *J. South China Univ. Technol. (Nat. Sci. Ed.)* **2022**, *50*, 84–92.
4. Alshaer, B.J.; Darabseh, T.T.; Momani, A.Q. Modelling and control of an autonomous articulated mining vehicle navigating a predefined path. *J. Int. J. Heavy Veh. Syst.* **2014**, *21*, 152–168. [\[CrossRef\]](#)
5. Ni, Z.; He, Y. Design and validation of a robust active trailer steering system for multi-trailer articulated heavy vehicles. *J. Veh. Syst. Dyn.* **2019**, *57*, 1545–1571. [\[CrossRef\]](#)
6. Pazooki, A.; Rakheja, S.; Cao, D. Kineto-dynamic directional response analysis of an articulated frame steer vehicle. *J. Int. J. Veh. Des.* **2014**, *65*, 060063. [\[CrossRef\]](#)
7. Xu, T.; Shen, Y.; Huang, Y. Study of hydraulic steering process for articulated heavy vehicles based on the principle of the least resistance. *J. IEEE/ASME Trans. Mechatron.* **2019**, *24*, 1662–1673. [\[CrossRef\]](#)
8. Bai, G.; Meng, Y.; Gu, Q. Relative navigation control of articulated vehicle based on LTV-MPC. *J. Int. J. Heavy Veh. Syst.* **2021**, *28*, 34–54. [\[CrossRef\]](#)
9. Huang, X.X.; Si, J.X.; Yang, J. Effect of mass bias of electrically driven articulated vehicle on steering stability. *J. Cent. South Univ. (Nat. Sci. Ed.)* **2017**, *48*, 2657–2664.
10. Morrison, G.; Cebon, D. Combined emergency braking and turning of articulated heavy vehicles. *J. Veh. Syst. Dyn.* **2017**, *55*, 725–749. [\[CrossRef\]](#)
11. Gao, Z.W.; Li, D.S.; Ye, L.Z. Study on braking stability of articulated vehicle of charged eddy current retarded axle. *J. Automot. Eng.* **2020**, *42*, 917–924.
12. Esmaeili, N.; Kazemi, R.; Tabatabaei, O.S.H. Design of a new integrated controller (braking and steering) to maintain the stability of a long articulated vehicle. *J. Proc. Inst. Mech. Eng. Part C J. Mech. Eng. Sci.* **2020**, *234*, 981–1013. [\[CrossRef\]](#)
13. Nie, Z.G.; Wang, W.Q.; Wang, C. Integrated control strategy for timely mode switching of medium and high speed heavy semi-trailers. *J. Transp. Eng.* **2017**, *17*, 135–149.
14. Zhang, C.; Hu, T.; Lin, X.C. Study on special slow lane for large trucks in continuous long downhill section of expressway. *J. South China Univ. Technol. (Nat. Sci. Ed.)* **2020**, *48*, 104–113.

15. Zhang, Y.; Khajepour, A.; Huang, Y. Multi-axle/articulated bus dynamics modeling: A reconfigurable approach. *J. Veh. Syst. Dyn.* **2018**, *56*, 1315–1343. [[CrossRef](#)]
16. Wang, W.W.; Zhao, Y.F.; Zhang, W. Yaw stability control strategy of multi-axle wheel-driven articulated passenger car. *J. Mech. Eng.* **2020**, *56*, 161–172.
17. Yang, S.Y.; Zeng, G.G.; Luo, Z.W. Simulation study on yaw stability control of multi-axis electrically driven vehicle. *J. Missile Space Deliv. Technol.* **2017**, *6*, 82–87.
18. Lei, T.; Wang, J.; Yao, Z. Modelling and stability analysis of articulated vehicles. *J. Appl. Sci.* **2021**, *11*, 3663. [[CrossRef](#)]
19. Morrison, G.; Cebon, D. Sideslip estimation for articulated heavy vehicles at the limits of adhesion. *J. Veh. Syst. Dyn.* **2016**, *54*, 1601–1628. [[CrossRef](#)]
20. Sorge, F. A nonlinear dynamical approach to the path correction of multi-steering articulated vehicles. *J. Veh. Syst. Dyn.* **2021**, *59*, 1759–1780. [[CrossRef](#)]
21. Rehnberg, A.; Drugge, L.; Trigell, A.S. Snaking stability of articulated frame steer vehicles with axle suspension. *J. Int. J. Heavy Veh. Syst.* **2010**, *17*, 119–138. [[CrossRef](#)]
22. Chen, X.; Chen, W.; Hou, L. A novel data-driven rollover risk assessment for articulated steering vehicles using RNN. *J. Mech. Sci. Technol.* **2020**, *34*, 2161–2170. [[CrossRef](#)]

Disclaimer/Publisher’s Note: The statements, opinions and data contained in all publications are solely those of the individual author(s) and contributor(s) and not of MDPI and/or the editor(s). MDPI and/or the editor(s) disclaim responsibility for any injury to people or property resulting from any ideas, methods, instructions or products referred to in the content.